International Journal of Information, Control and Computer Sciences
ISSN: 2517-9942
Vol:1, No:12, 2007

The Use of Complex Contourlet Transform on Fusion Scheme

Dipeng Chen, and Qi Li

Abstract**—**Image fusion aims to enhance the perception of a scene by combining important information captured by different sensors. Dual-Tree Complex Wavelet (DT-CWT) has been thouroughly investigated for image fusion, since it takes advantages of approximate shift invariance and direction selectivity. But it can only handle limited direction information. To allow a more flexible directional expansion for images, we propose a novel fusion scheme, referred to as complex contourlet transform (CCT). It successfully incorporates directional filter banks (DFB) into DT-CWT. As a result it efficiently deal with images containing contours and textures, whereas it retains the property of shift invariance. Experimental results demonstrated that the method features high quality fusion performance and can facilitate many image processing applications.

Keywords**—**Complex contourlet transform, Complex wavelet transform, Fusion.

I. Introduction

FUSION scheme has been explored in a wide range of research fields, including *computer vision*, *automatic object detection*, *parallel and distributed processing*, and *robotics remote sensing*. In general a successful fusion should extract complete information from source images into the result, without introducing any artifacts or inconsistencies. Many algorithms developed so far can be classified into three primary categories: *spatial-domain*, *transform-domain* and *optimization methods*, as illustrated in Figure 1.

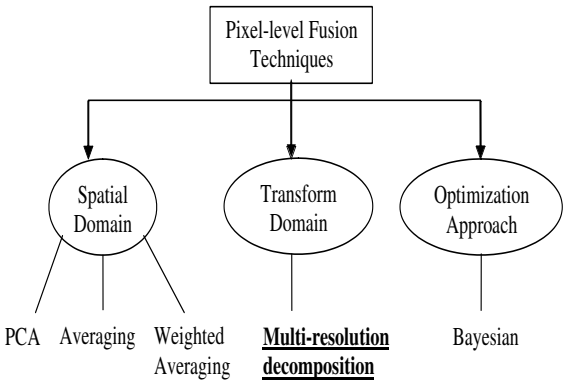

Fig. 1. The classification of pixel-to-pixel based image fusion methods

Primitive fusion schemes, such as averaging, weighted averaging and global Principal-Component-Analysis (PCA), are performed solely in the spatial domain. In spite of easy implementation, these methods pay the expenses of reducing the contrast and distorting the spectral characteristics [1]. To solve these problems, some more sophisticated fusions in the transform domain gather tools like multi-resolution decomposition (MR). It decomposes images at different scale to several components, which account for important salient features of images [1]. Therefore it enables a better performance than those performed in the spatial domain. On the other hand, methods in the third category utilizes Bayesian optimization to find the fused image, however, it suffers from a significant increase of computational complexity [2-3].

In this paper, we confine our discussion to MR approaches; motivated by the fact that the human visual system is primarily sensitive to local contrast changes, i.e. edges. Assume a source image is decomposed with perfect reconstruction [1] to several sub-parts by *operator* $T\{\cdot\}$, a fusion rule is then applied onto each sub-part to construct a combined representation, and a fused image is finally obtained by performing the inverse decomposition process $T\{\cdot\}^{-1}$. Wavelet is a well-known choice of the transform $T\{\cdot\}$ for fusion. It is, however, not suited for the application with mis-registration, due to the severe problem of shift dependence. As an alternative, DT-CWT scheme [8] provides the approximate shift invariance which the traditional wavelet transform is short of. But it also suffers from the drawback of limited directional information, and takes into account no correlation of significant wavelet coefficient along the discontinuity curve. As a result a poor representation of edges is produced, particularly when images have contours and curves.

Hence, a new transform *Complex Contourlet transform* is proposed, which incorporates the DT-CWT and DFB to provide a flexible and robust scale-direction representation for source images. Specifically the flexibility allows arbitrary number of directions at any scale, which can help to capture most important salient information in images, i.e. edges. Whereas the robustness refers to a shift-invariance of the proposed method that could yield a fusion free of aliasing. CCT is therefore well-suited to image fusion scheme, as it provides simultaneous better directional sensitivity and shift invariance.

The organization of rest of the paper is as follows. Section II describes the preliminary analysis of the CCT for image fusion. A new fusion scheme using CCT is subsequently proposed in Section III. Following that, experimental results of the proposed method, in both visual and quantity aspects, are compared to the other traditional methods in Section IV. Section V presents the conclusions.

II. The Complex Contourlet Transform

A. Algorithm

The complex contourlet transform consists of two subsequent stages. Firstly we allow a complex dual-tree wavelet decomposition, in contrast to the critically sampled DWT used in [12], and Laplacian Pyramid used in [4]. After applying DT-CWT decomposition, the detail subspace W_j at the scale 2^j contains a structure of dual-trees, and thus gives rise to six subbands, formulated as follows, rather than conventional LH, HL and HH subbands, indexed by $i \in \{1, 2, 3\}$.

$$\{\gamma^i_{\mathbf{m},u,v}(\mathbf{t})\}_{\mathbf{m},\mathbf{t}\in Z^2} \quad (1)$$

Dipeng Chen is with the London Business School, London, United Kingdom (corresponding author to provide phone: 44-20-7262-5050; fax: 44-20-7724-7875; e-mail: dipengchen.phd2004@london.edu).
Qi Li, is with Imperial College London, United Kingdom.

$i \in \{1,2,3\}$ and $u \in \{1,2\}$ reveals where the coefficient at location index **t** originates from. The six subbands at each scale capture distinct directions, whereas each of them has two wavelets, specified by $v \in \{1,2\}$ as real and complex part of wavelet coefficients. **m** denotes a location shift. The detail subspace W_j is turned into an approximate shift invariance [8] by averaging outputs of dual trees.

However, these subbands with fixed orientation are still not enough. The solution is to apply the l_j levels' DFB to each multiscale detail space W_j, and the subbands hence can be expanded to the number of 2^{l_j}, as defined in the following mathematical form:

$$\mu^{i,l_j}_{k,\mathbf{n},u,v}(\mathbf{t}) = \sum_{\mathbf{m}\in Z^2} g^{l_j}_k[\mathbf{m} - S^{l_j}_k \mathbf{n}]\gamma^i_{\mathbf{m},u,v}(\mathbf{t}) \qquad i = 1,2,3 \qquad (2)$$

It is easy to see that $\mu^{i,l_j}_{k,\mathbf{n},u,v}(\cdot)$ represents a family of directional subspace $W^{l_j}_{j,k}$ at the scale 2^j and a decomposition direction $k = 1...2^{l_j}$. In addition, $g^{(l_j)}_k(\cdot)$ expresses the impulse response of the synthesis filter, and its translated version over the sampling lattices $S^{l^j}_k$ is denoted by $g^{l_j}_k[\mathbf{m} - S^{l_j}_k \mathbf{n}]$.

In this case, each directional subspace $W^{l_j}_{j,k}$ consists of a complex double tree like frame with many more flexible directions than W_j of DT-CWT. We refer to this kind of transform as Complex Contourlet Transform (CCT). Obviously it is a better choice for fusion scheme than DT-CWT, as the former can extract more directions from images and produce a better representation of local features, such as smooth edges.

B. Shift Dependence of the Algorithm

Concerning the particular importance of shift invariance for fusion, it is necessary at this stage to explore the robustness of CCT.

W_j of DT-CWT is nearly shift invariant [2], and this property can be still established in the subspace $W_{j,k}$, even after applying directional filter banks on detail subspace W_j. We denote the scaling function at the scale of 2_jbefore the processing of DFB as follows:

$$\gamma^i_{\mathbf{m},u,v}(\mathbf{t}) = 2^{-j}\gamma^i(\frac{\mathbf{t} - 2^j\mathbf{m}}{2^j}) \qquad t,m \in Z^2 \text{ and } i = 1,2,3 \quad (3)$$

A small shift in pixel locations $\mathbf{m}'$ gives the following relationship:

$$\gamma^i_{\mathbf{m}+\mathbf{m}',u,v}(\mathrm{t}) = \gamma^i_{\mathbf{m},u,v}(\mathbf{t} - 2^j\mathbf{m}') \qquad i = 1,2,3 \qquad (4)$$

Therefore, the subbands of CCT are derived by direct substitutions:

$$\mu^{i,l_j}_{\mathbf{m},u,v}(\mathbf{t}) = \sum_{m\in Z^2} g^{l_j}_k[\mathbf{m} - S^{l_j}_k \mathbf{n}]\gamma^i_{\mathbf{m},u,v}(\mathbf{t}) \qquad (5)$$

$$= \sum_{m\in Z^2} g^{l_j}_k[\mathbf{m}]\gamma^i_{\mathbf{m},u,v}(\mathbf{t} - 2^j S^{l_j}_k \mathbf{n}) = \mu^{i,l_j}_{\mathbf{m},u,v}(\mathbf{t} - 2^j S^{l_j}_k \mathbf{n}) \qquad (6)$$

As a result the subspaces $W^{l_j}_{j,k}$ are established to satisfy the property of the shift invariance, since they are generated by a single function and its translations [4-5].

$$f(\mathbf{t}) \in W^{l_j}_{j,k} \Leftrightarrow f(\mathbf{t} - 2^j S^{l_j}_{k,j}) \in W^{l_j}_{j,k} \qquad t \in Z^2 \qquad (7)$$

Moreover, the proposed method guarantees perfect reconstruction due to that both DT-CWT and DFB are. This means the input image can be therefore reconstructed by corresponding subband images without loosing any important information.

Figure 2 demonstrates the complete procedure of the CCT, which uses the complex wavelet to capture as much as salient information as possible , followed by a directional filter bank to group those locally correlated coefficients into smooth structures. Unlike the other wavelet transform, CCT allows for at each scale arbitrary directions, as well as approximate shift invariance. Therefore it could efficiently facilitate the fusion of geometric (spatial) and thematic (spectral) features from source images, in particular it sharpens contours and smooth edges.

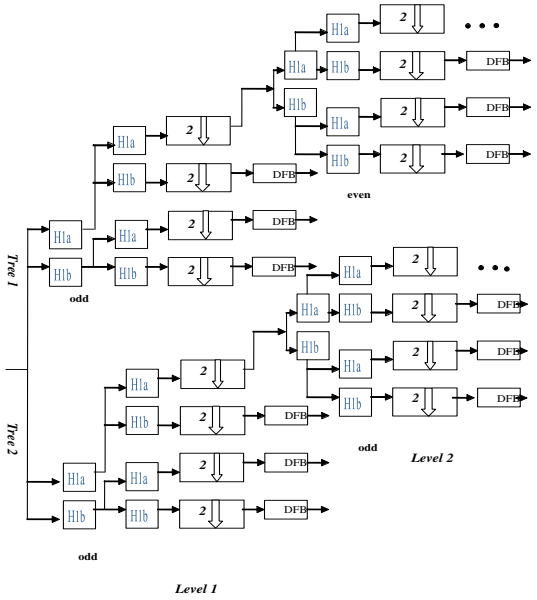

Fig. 2. The procedure of the complex contourlet transform (CCT)

III. The CCT Fusion Scheme

Similar to the wavelet-based fusion, the CCT based fusion consists of three stages. The first stage provides a sub-band and directional decomposition by applying the proposed transform. It is followed by applying various fusion rules onto the transform coefficients at the second stage. A simple and effective one, we used in this paper, choose the complex coefficients with maximum magnitudes. The choosing-maximum scheme is a popular choice as we tend to pick out the salient features of an image, e.g. edges and boundaries. The complete fusion schemes ends with the inverse complex contourlet transform, as shown in Figure 3.

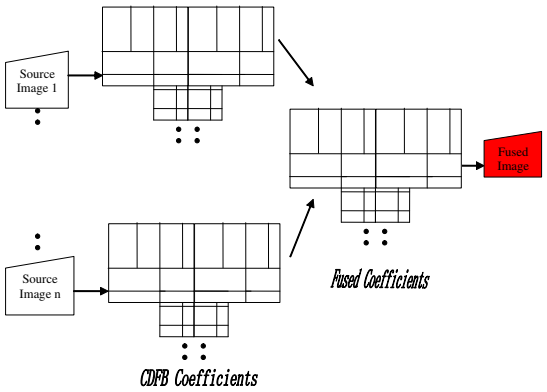

Fig. 3. The proposed fusion scheme using complex contourlet transform

IV. Experimental Study and Analysis

Visual and quantitative comparisons are two major means to evaluate the quality of distinct fusion schemes. In this section, we compare the proposed method with the other conventional ones in terms of both visual and quantitative measurements, under the assumption of all the sources images are geometrically registered to each other.

A. Visual Analysis

Quality assessment of our proposed algorithm is first carried out by the visual inspection, under the assumption that all the source images are registered. In Figure 4 (c-f), we display all the fusion results obtained by applying principle component analysis (PCA), shift invariant discrete wavelet transform (SI-DWT), DT-CWT and CCT respectively. It was observed that Figure 4 (d), fused by SI-DWT, is closest to the original visual image, as shown in Figure 4 (a) , but farthest to the multi-spectral image in Figure 4 (b). On the contrary, Figure 4 (c) illustrates a considerable spatial distortion present in the PCA based fusion, although the spectral information is well retained. In contrast to Figure 4 (c) and (d), the fusions obtained by the DT-CWT and CCT transform have both high spatial resolution, similar with the Figure 4 (a), and same rich spectral information as the Figure 4 (b). Moreover, the proposed fusion Figure 4 (e) reveals slightly more enriched geometric structure and less disturbing artifacts than DT-CWT based fusion. Hence in terms of visual interpretation, the fused image obtained by CCT-based fusion is optimal for a better visual effect, such as contrast enhancement around edges.

As it is recognized, visual comparison is not sufficient to reveal the exact potential of the fusion method [9]. Therefore, statistical comparison is attempted to further evaluate the fusion results. It is believed that such a comparison in the next section would accurately assess the quality of the fused image.

B. Quantitative Measurements

The CCT transform that we used in our experiments decomposes an image into 5 levels using the 9-7 biorthogonal Daubechies (wavelet) transform, where each sub-band at each level is fed to the directional banks stage with eight directions at the finest level. In the DFB stage, we use the 23-45 biorthogonal quincunx filters designed by [16] and modulate them to obtain the biorthogonal fan filters. For comparison, we implemented in a similar fashion as in the visual assessment, a PCA based fusion, SIDWT based fusion and DT-CWT based fusion , which are decomposed to 5 levels.

Several objective quantitative assessments [10] were considered for assessing the spectral and spatial quality of the fused images. Most conventional objective assessments require a ground-truth image f as a reference, such as *Correlation Coefficient (CC)* that are widely used in many disparate applications. However, due to the lack of ground truth in practice, a more reliable and flexible choice is to use the *Mean Gradient (MG)*, *Average Value (AV)*, as presented in [6,13-15].

1) The *correlation coefficient (CC)* is defined as

$$Corr(f,\widehat{f}) = \frac{\sum_{m,n}(f_{mn}-\overline{f})(\widehat{f}_{mn}-\overline{\widehat{f}})}{\sqrt{(\sum_{m,n}(f_{mn}-\overline{f})^2)(\sum_{m,n}(\widehat{f}_{mn}-\overline{\widehat{f}})^2)}} \quad (8)$$

where $\widehat{f}$ is the fused image, and $\overline{f}$ and $\overline{\widehat{f}}$ stand for the mean of the original and fused image. Correlation coefficient ranging from -1 to +1 indicates the amount of spectral content preserved in the fused image [9]. Larger correlation coefficients illustrate that more spectral content in the fused image is similar to the initial multi-spectral image.

2) On the other hand, the mathematical definition of *mean gradient (MG)* is :

$$MG(\widehat{f}) = \frac{1}{MN}\sum_{i=1}^{M}\sum_{j=1}^{M}\sqrt{(\Delta I_x^2 + I_y^2)/2} \quad (9)$$

$\Delta I_{x;i,j} = f(i+1,j) - f(i,j), \Delta I_{x;i,j} = f(i,j+1) - f(i,j)$ where M and N are the pixel number of an image f in the row and column respectively. MG of the fused image simply reflects the contrast between the detailed variation of patter on the image and clarity of the image [11-15].

Besides, *average (AV)* is also a sound indicator for spatial resolution.

Table I presents the experimental results using the PCA based fusion, DT-CWT based fusion and CCT transform based fusion schemes, in terms of the mean gradient, correlation coefficient and average values.

TABLE I
PERFORMANCE COMPARISON FOR THE PCA, SIDWT, DT-CWT AND CCT FUSION METHODS

Methods	MG	CC	AV
visual image	N/A	N/A	**80.2766**
multispectral image	N/A	N/A	77.7234
PCA	724.6968	0.8446	78.6876
SIDWT	1091	0.8803	79.0012
DT − DWT	1147.9	0.8952	80.1860
CCT	**1147.9**	**0.9166**	**80.2766**

It is evident to see from the Table I that the resulting image from CCT based fusion has better spectral quality than the other methods, in terms of the higher values of correlation coefficient and mean gradient. As far as the spatial resolution is concerned, the average value of the proposed method is same as the spectral image, while DT-CWT based fusion is the next best. Thus the result obtained by CCT based fusion has the identical grayscale distributions to the original visual image. Whereas, its geometric quality is better than the others obtained by conventinal schemes, in terms of a better representation of edges and contours is yielded. The conclusion accords with our observation in Figure 5 between high-pass filter outputs of fused images. The highest value of correlation coefficient **0.8644** in this case indicates that most geometric details are enhanced in the image fused by CCT transform.

As it could be seen from the preceding experimental results, CCT based fusion approach is the optimum and most well-suited to remote sensing application, in terms of the spectral and spatial quality.

V. SUMMARY AND CONCLUSIONS

In this work, we have propsed a *complex contourlet transform* for image fusion. The motivation to apply the new transform is that it provides a flexible and shift-invariant sparse expansion of image, which enables both high spatial and spectral resolutions. After presenting a comparison of fused images obtained by the PCA, SIDWT, DT-CWT and CCT, it is concluded that the proposed method outperforms the other complex wavelet based methods and PCA based method. It can well adapt to the application of fusing remote sensing images, e.g. IKONS, SPOT, Landsman.

REFERENCES

[1] G. Piella, “A general framework for multi-resolution image fusion: from pixels to regions,” PNA-R0211, ISSN 1386-3711, 2002.
[2] B. Jeon and D. A. Landrebe, “Decision fusion approach for multitemporal classification,” IEEE Transactions on Geoscience and Remote Sensing, vol. 37, no. 7, pp. 1227-1233, 1999.
[3] R. K. Sharma and M. Pavel, “Adaptive and statistical image fusion,” Society for information Display Digest of Technical Papers, vol. 27, pp. 969-972, 1996.
[4] M. N. Do and M. Vetterli, “Contourlets:A directional multi-resolution image representation”, Proc. of IEEE intl. Conf. on Image Processing, Rochester, September 2002.
[5] M. N. Do and M. Vetterli, “Contourlets,” *Beyond Wavelets*, Academic Press, New York, 2003.
[6] Z. Wang and A. C. Bovik, “A universal image quality index,” *IEEE Signal Processing Letters*, vol. 9, no. 3, pp. 81-84, March 2002.
[7] Paul. R. Hill, C. N. Canagarajah, D. R. Bull, “Image fusion using complex wavelets”. BMVC 2002.
[8] N. G. Kingsbury, “Shift invariant properties of the dual-tree complex wavelet transform,” Proc. IEEE Int. Conf. Acoust., Speech, Signal Process. ICASSP ’99, March 1999.
[9] S. Sanjeevi, K. Vani and K. Lakshmi “Comparison of conventional and wavelet transform techniques for fusion of IRS-1C LISS-III and PAN Images,” 22nd Asian Conference on Remote Sensing, Singapore, November 2001.

[10] A. R. Afary “Application of Wavelets Transform in Optimization of satellite Image Fusion”, Master of Science Thesis, 2002.
[11] P. J. Burt and A. E. Adelson, “The Laplacian pyramid as a compact image code”, IEEE Trans. on Communications, vol. 31, pp. 532-540, 1983.
[12] R. Eslami and H. Radha, “Wavelet-based contourlet transform and its application to image coding”, IEEE intl. Conf. on Image Processing, 2004.
[13] L. Wald, T. Ranchin and M. Mangolini, “Fusion of Satellite images of difference spatial resolution: Assessing the quality of resulting images,” Photogrammetric Engineering and Remote Sensing, vol. 63, no. 6, pp. 691-699, 1997.
[14] J. Li and Z. J. Liu, “Data fusion for remote sensing imagery based on feature,” China Jounal of Remote Sensing, vol. 2, no. 2, pp. 103-107, 1998.
[15] W. Z. Shi, C. Q. Zhu, C. Y. Zhu and X. M. Yang, “Multi-Band wavelet for fusion SPOT Panchromatic and multispecteral images,” Photogrammetric Engineering and Remote Sensing, vol. 69, no. 5, pp. 513-520, 2003.
[16] J. B. Sun, J. L. Liu and J. Li, “Multi-source remote sensing image data fusion,” China Jounal of Remote Sensing, vol. 2, no. 1, pp. 47-50, 1998. S. M. Phoong, C. W. Kim, P. P. Vaidynathan, and R. Ansari, “A new class of two-channel biorthogonal filter banks and wavelet bases,” IEEE Trans. Signal Proc., vol. 43, no. 3, pp. 649-665, March 1995.

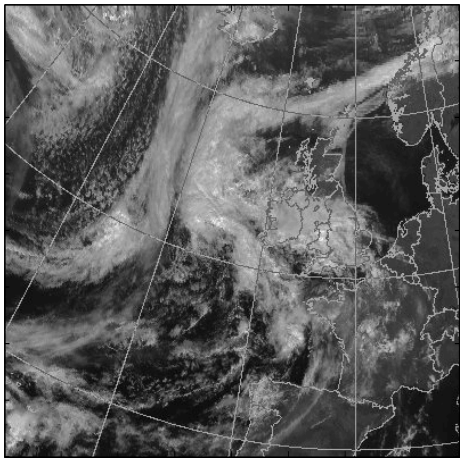

(a) Original visual image

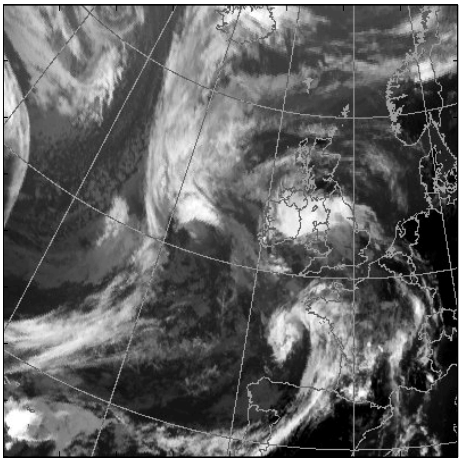

(b) Original multispectral image

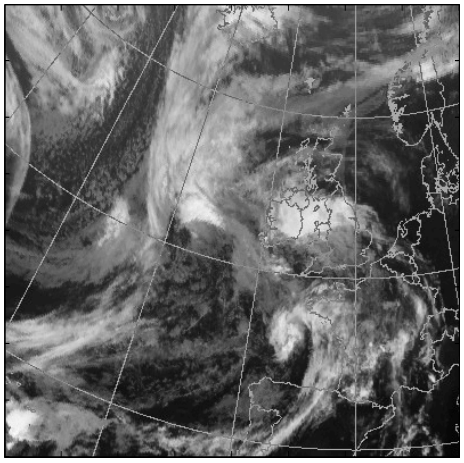

(c) Image fused by Principal Component Analysis

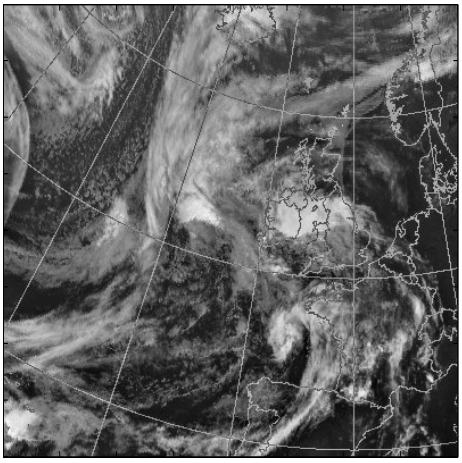

(d) Image fused by Shift-invariant Discrete Wavelet Transform

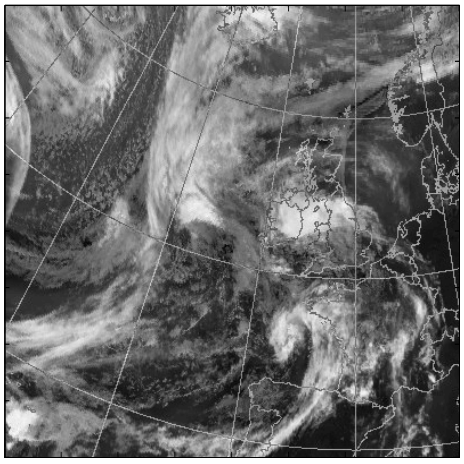

(e) Image fused by Dual-tree Complex Wavelet Transform

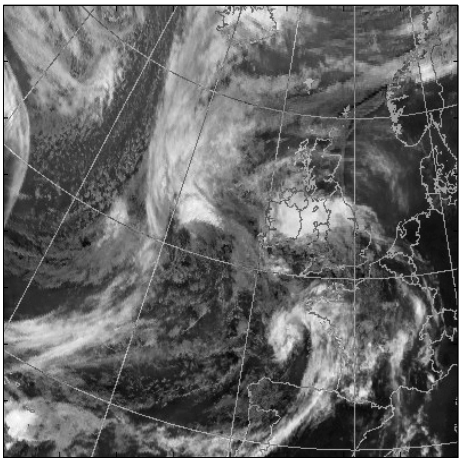

(f) Image fused by Complex Contourlet Transform

Fig. 4. Performance comparison of fusing the remote sensing images using four different methods including PCA, SIDWT, DT-CWT and CCT

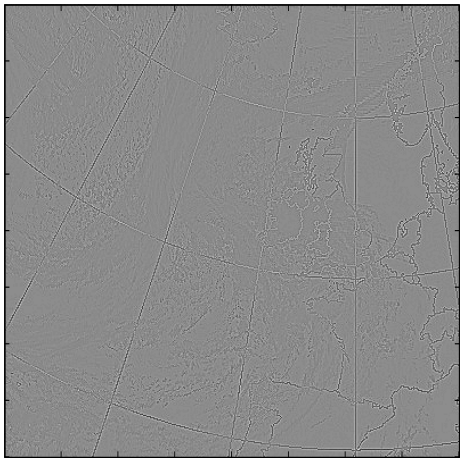

(a) Original high-pass visual image

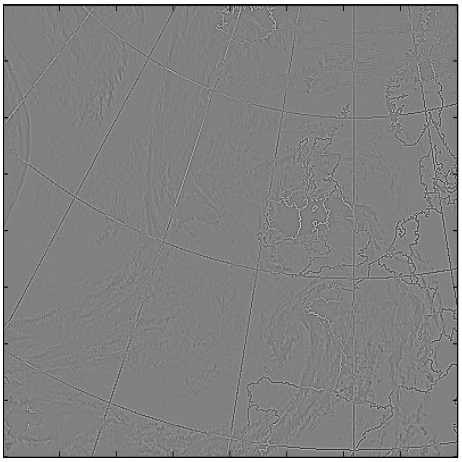

(b) Original high-pass multispectral image

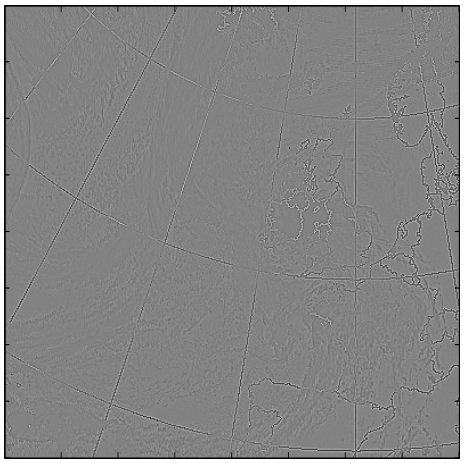

(c) High-pass image fused by Principal Component Analysis with correlation coefficient equal to 0.8493

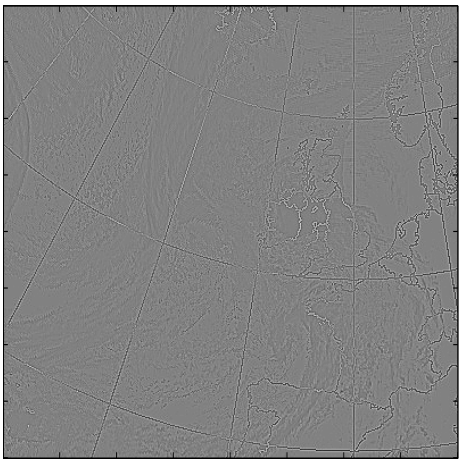

(d) High-pass image fused by Shift-invariant Discrete Wavelet Transform with correlation coefficient equal to 0.8626

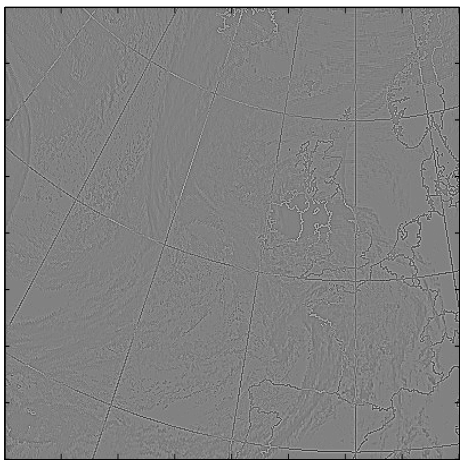

(e) High-pass image fused by Dual-tree Complex Wavelet Transform with correlation coefficient equal to 0.8637

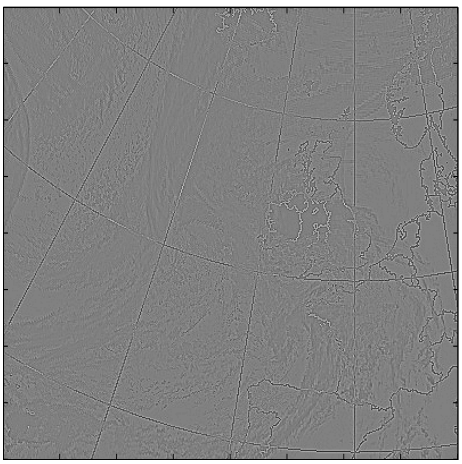

(f) High-pass image fused by Complex Contourlet Transform with correlation coefficient equal to **0.8644**

Fig. 5. Comparison of high pass filtered image after fusing remote sensing images using four different methods including PCA, SIDWT, DT-CWT and CCT